

Article

**Self-Assembly by Mutual Association: Basic Thermodynamic Properties**

Jacek Dudowicz, Jack F. Douglas, and Karl F. Freed

*J. Phys. Chem. B*, **2008**, 112 (50), 16193-16204 • DOI: 10.1021/jp806859w • Publication Date (Web): 14 November 2008

Downloaded from <http://pubs.acs.org> on January 6, 2009

**More About This Article**

---

Additional resources and features associated with this article are available within the HTML version:

- Supporting Information
- Access to high resolution figures
- Links to articles and content related to this article
- Copyright permission to reproduce figures and/or text from this article

[View the Full Text HTML](#)

# Self-Assembly by Mutual Association: Basic Thermodynamic Properties<sup>†</sup>

Jacek Dudowicz,<sup>\*,‡</sup> Jack F. Douglas,<sup>§</sup> and Karl F. Freed<sup>‡</sup>

The James Franck Institute and the Department of Chemistry, The University of Chicago, Chicago, Illinois 60637, and Polymers Division, National Institute of Standards and Technology, Gaithersburg, Maryland 20899

Received: July 31, 2008; Revised Manuscript Received: September 26, 2008

Many natural and synthetic self-assembly processes involve the mutual association of molecules or particles with complementary interactions (e.g., antigen–ligand binding of proteins), which in turn polymerize into larger scale structures. We develop a systematic Flory–Huggins type theory for this hierarchical assembly by combining descriptions of the mutual association of the molecular and particle species A and B and the subsequent polymerization of the  $A_pB_q$  complexes. In particular, basic thermodynamic properties (order parameter, concentration profiles, average cluster mass, etc.) are computed for the mutual assembly process as a function of temperature, the initial relative composition of A and B, solvent concentration, and the ratio of the stoichiometric indices  $p$  and  $q$ . Calculations are performed for the single-step (i.e., without subsequent polymerization) and multistep mutual association models. The main characteristics found for these mutually associating systems are compared to those reported previously by us for self-association. For instance, we find that the average cluster size (mass) becomes considerably enhanced at the “critical” stoichiometric volume fraction  $(\phi_\lambda^c)^* = p/(p + q)$ , consistent with the observation of a peak in the shear viscosity of mutually associating fluid mixtures exhibiting polymerization at equilibrium.

## I. Introduction

Many processes in living systems and in synthetic complex fluids involve the mutual association between distinct chemical species.<sup>1,2</sup> The binding of oxygen to hemoglobin is a classical, well studied, example of this phenomenon.<sup>3–6</sup> The selectivity to molecular structure (size, shape, and chemical interactions) can be exquisite, a typical characteristic of a complementary association phenomenon that Emil Fisher<sup>7</sup> has described in terms of a lock and key paradigm. Selective association also underlines diverse switching processes<sup>8,9</sup> that are essential to life and to the faithful replication of genetic information in the biosynthesis of macromolecules. The immune system of higher organisms relies on molecular recognition through the formation of ligand–antigen association complexes.<sup>10</sup> Many drugs act by competing with natural ligand–antigen association processes.<sup>11</sup> By extension, recent interest centers on developing biomimetic, synthetic ligand–receptor systems<sup>12</sup> (for selective molecular recognition and encapsulation<sup>13</sup>), synthetic nanoparticle assemblies,<sup>14–20</sup> and responsive materials.<sup>21</sup>

In addition to the association of species with complementary interactions, hierarchical structures form in many self-assembling systems by the mutual association of complex or “protamer” species. This ubiquitous phenomenon is illustrated by the organization of ligand–antigen complexes into supermolecular chainlike structures,<sup>22</sup> the organization of clathrin molecules about a central hub molecule, followed by the organization of these triskelion (three-arm stars) into closed clathrin cages that are essential for the translocation of nanoparticle structures across cell membranes.<sup>23–25</sup> The self-assembly of many spherical (icosahedral) viruses also occurs through the initial formation of pentamer and hexamer protein clusters that comprise the basic (“protamer”) subunits of the capsid shell.<sup>26</sup> Complexes between

cholesterol and phospholipids, such as sphingomyelin, are believed to produce “raft” structures in the membranes of animal cells,<sup>27</sup> structures that provide platforms for a wide range of biological activities. Numerous recent studies in materials science reveal the formation of a supermolecular assembly of molecules having complementary donor and acceptor hydrogen bond interactions, systems which likewise self-assemble into large linear or branched chain supermolecular molecules whose dimensions are tunable by changing temperature or other thermodynamic variables.<sup>28–34</sup> Systems exhibiting mutual association do not require exotic chemistry, and indeed, association is prevalent in many alcohol and alcohol–water mixtures, mixtures involving hydrogen bonding or polar molecules, or mixtures of organic compounds with chlorinated hydrocarbons.<sup>35–42</sup> Other mutual association processes include counterion binding in polyelectrolytes,<sup>43</sup> ionic solutions,<sup>44</sup> and ionomers,<sup>45</sup> ligand binding to polymers,<sup>46</sup> and the hydration of water soluble polymers.<sup>47</sup> Mutual association is also expected to be present in diverse self-assembly processes occurring in mixtures of anionic and cationic surfactants.<sup>48</sup>

In the present work, we formulate a simple Flory–Huggins type theory for the thermodynamics of self-assembly by *mutual association*. Specifically, we describe the mutual association of two distinct species A and B into the complex  $A_pB_q$ . Many different mechanisms exist for forming the  $A_pB_q$  complexes because of the variability of possible inter- and intramolecular associative contacts.<sup>49</sup> Here, we adopt a simple coarse-grained model that addresses generic characteristics of the coupling between assembly of the complexes and their subsequent polymerization (an approach that can be specialized to treat more detailed structures<sup>49</sup>). Even within our simplified model, the coupling between mutual association and the larger scale polymeric assembly leads to association processes with variable degrees of cooperativity<sup>49,50</sup> (as discussed below). Since mass action constraints on mutual association differ considerably from those governing self-association, the thermodynamics of the

<sup>†</sup> Part of the “Karl Freed Festschrift”.

<sup>‡</sup> The University of Chicago.

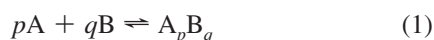
<sup>§</sup> National Institute of Standards and Technology.

mutual self-assembly process departs greatly from that of ordinary equilibrium polymerization. For example, the composition of the complex  $A_pB_q$ , extent of polymerization  $\Phi_p$ , and average cluster size  $L$  peak at a critical stoichiometric concentration that depends on the ratio  $p/q$  (see below). Such strong peaks have long been observed in the transport properties (low frequency dielectric constant, shear viscosity, etc.) of fluids exhibiting strong mutual association (including many alcohol mixtures and mixtures of alcohols with water). Likewise, mutually associating complexes between polymer chains have been suggested to underlie the toughness of gels of interest for medical applications.<sup>51,52</sup> Our simple theoretical formulation of mutual association is expected to provide insight into a wide range of natural and synthetic assembly processes involving complementary particle association.

Section II describes the theoretical background of mutual association between the A and B species and the subsequent formation of polymer structures  $\{A_pB_q\}_i$ . Illustrative calculations for basic thermodynamic properties are summarized and discussed in section III.

## II. Flory–Huggins Theory of Mutual Association

**A. Single-Step Model of Mutual Association.** The simplest model of *mutual association* is described by the general equation



in which  $p$  molecules of species A react with  $q$  molecules of species B, forming a complex  $A_pB_q$  in equilibrium. Special cases of eq 1 have long been considered as models of complex formation in associating fluids (e.g., see ref 37), and the general model defined by eq 1 has been advocated to describe complex formation between cholesterol and phospholipids in membranes.<sup>27,53</sup> The chemical equilibrium constant for the reaction in eq 1 is

$$K = \exp[-(\Delta h - T\Delta s)/(k_B T)] \quad (2)$$

where  $\Delta h$  and  $\Delta s$  are the enthalpy and the entropy of the mutual association process,  $T$  is the absolute temperature, and  $k_B$  is Boltzmann's constant. Before association, the system consists of  $n_A^0$  and  $n_B^0$  molecules of the associating species A and B, respectively, along with  $n_s$  solvent molecules which do not participate in the association process. All molecules of species A and B and solvent are represented within the lattice model as occupying single lattice sites, whereas each cluster  $A_pB_q \equiv C$  extends over  $p + q$  lattice sites. A fundamental treatment of mutual association ( $A + B \rightleftharpoons AB$ ) in the gas phase by Olausson and Stell<sup>54</sup> provides insights into the concentration dependence of the equilibrium constant that arises from nonassociative interactions.

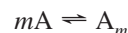
Classic Flory–Huggins theory treats the system as incompressible with constant volume. The constant volume condition implies a fixed total number of lattice sites  $N_1$

$$N_1 = n_s + n_A^0 + n_B^0 = n_s + n_A + n_B + (p + q)n_C \quad (3)$$

where  $n_\alpha$  ( $\alpha \equiv A, B, C$ ) is the number of molecules of type  $\alpha$  in equilibrium. The composition of the system (before association) is uniquely determined by the pair of the volume fractions  $\phi_A^0 \equiv n_A^0/N_1$  and  $\phi_B^0 \equiv n_B^0/N_1 = 1 - \phi_A^0 - \phi_s$ , where  $\phi_s \equiv n_s/N_1$  denotes the volume fraction of the solvent. The two independent volume

fractions ( $\phi_A^0$  and  $\phi_B^0$ ), along with the absolute temperature  $T$  and the free energy parameters  $\Delta h$  and  $\Delta s$  of the reaction in eq 1, constitute the set of essential intensive thermodynamical variables characterizing the self-assembly process. Thus, the three equilibrium concentrations  $\phi_A$ ,  $\phi_B$ , and  $\phi_C$  (as well as other basic thermodynamic properties, such as the extent of polymerization, the average cluster size, the association transition line, etc.) are expressible in terms of these intensive variables. It is sometimes convenient to introduce the alternative independent composition variables, the normalized volume fraction  $\phi_{A,n}^0 \equiv \phi_A^0/(1 - \phi_s)$  [ $\phi_{B,n}^0 \equiv \phi_B^0/(1 - \phi_s) = 1 - \phi_{A,n}^0$ ] and the solvent composition  $\phi_s$ .

The model of mutual assembly in eq 1 is a natural extension of the  $\mathcal{F}Am$  model of self-assembly



which was originally introduced by Debye to describe the self-assembly of micelles.<sup>55</sup> We have shown<sup>50</sup> that the “cooperative” assembly of the  $\mathcal{F}Am$  model is essentially equivalent to a chain of sequential association processes involving particles that are subject to regulatory constraints, such as thermal activation or chemical initiation. Both the  $\mathcal{F}Am$  model and its mutual association analog ( $\mathcal{M}A_{pq}$ ) of the present paper should likewise be considered as “coarse-grained” reaction schemes rather than molecularly faithful representations of real association–dissociation processes. Clearly, the idea that some large number of molecules ( $p$ ) simultaneously reacts with a large number of another kind of molecules ( $q$ ) should not be taken literally. Hill provides a systematic description of a more realistic mechanism for the formation of the associated complexes  $A_pB_q$ .<sup>2</sup>

The Helmholtz free energy for the associating system is expressed as

$$\begin{aligned} \frac{F}{N_1 k_B T} = & \phi_s \ln \phi_s + \phi_A \ln \phi_A + \phi_B \ln \phi_B + \\ & \frac{\phi_C}{p + q} \ln \phi_C + \phi_C f_C + 2\phi_A \phi_B \chi_{AB} + \phi_A^2 \chi_{AA} + \phi_B^2 \chi_{BB} + \\ & 2\phi_A \phi_C \chi_{AC} + 2\phi_B \phi_C \chi_{BC} + \phi_C^2 \chi_{CC} + 2\phi_s \phi_A \chi_{As} + \\ & 2\phi_s \phi_B \chi_{Bs} + 2\phi_s \phi_C \chi_{Cs} + \phi_s^2 \chi_{ss} \quad (4) \end{aligned}$$

where  $\{\chi_{\alpha\beta} \propto 1/T\}$  are the interaction parameters between monomers of species  $\alpha$  and  $\beta$  ( $\alpha, \beta \equiv A, B, C, s$ ) and  $f_C$  is the specific free energy of complex C that emerges from FH theory for linear polymer chains as

$$f_C = \frac{1}{p + q} \ln \frac{2\gamma^2}{z(p + q)} + \frac{p + q - 1}{p + q} - \ln \gamma + \frac{1}{p + q} \frac{\Delta h - T\Delta s}{k_B T} \quad (5)$$

with  $z$  being the lattice coordination number,  $\gamma$  designating the stiffness parameter (equal to 1 for rigid chains and  $z - 1$  for fully flexible chains), and  $\Delta h$  and  $\Delta s$  denoting the free energy parameters of the reaction in eq 1. The specific free energies  $f_A$ ,  $f_B$ , and  $f_s$  are taken in eq 4 as vanishing identically, since both solvent and monomers of species A and B are treated as entities occupying single lattice sites. A disparity in the sizes of species and compressibility effects can also be incorporated into the theory.<sup>56</sup> The phase behavior of mutually associating systems is extremely rich and will be addressed elsewhere.

The condition of chemical equilibrium imposes a relation between the chemical potentials  $\mu_A$ ,  $\mu_B$ , and  $\mu_C$  of the A, B, and C species, respectively,

$$\mu_C = p\mu_A + q\mu_B \quad (6)$$

Calculating the chemical potentials  $\{\mu_\alpha\}$  ( $\alpha \equiv A, B, C$ ) directly from the free energy in eq 4 and inserting the resulting expressions into eq 6 yields

$$\phi_C = \frac{z(p+q)\gamma^{p+q-2}}{2} \phi_A^p \phi_B^q K \exp[2\phi_A(\chi_A - \chi_C) + 2\phi_B(\chi_B - \chi_C) + 2\phi_s(\chi_s - \chi_C) + 2\chi_C] \quad (7)$$

where

$$\chi_A \equiv p\chi_{AA} + q\chi_{AB} - (p+q)\chi_{AC} \quad (8)$$

$$\chi_B \equiv q\chi_{BB} + p\chi_{AB} - (p+q)\chi_{BC} \quad (9)$$

$$\chi_C \equiv p\chi_{AC} + q\chi_{BC} - (p+q)\chi_{CC} \quad (10)$$

$$\chi_s \equiv p\chi_{As} + q\chi_{Bs} - (p+q)\chi_{Cs} \quad (11)$$

and the equilibrium constant  $K$  is defined by eq 2. Equation 7 enables determining  $\phi_C$  (for a given  $\phi_A^\circ$  and  $\phi_B^\circ$ ) provided that  $\phi_A$  and  $\phi_B$  are known as a function of  $\phi_C$ . The latter requisite information emerges from the mass conservation conditions

$$\phi_A^\circ = \phi_A + \frac{p}{p+q}\phi_C \quad (12)$$

and

$$\phi_B^\circ = \phi_B + \frac{q}{p+q}\phi_C \quad (13)$$

Solution for  $\phi_C$  can only be determined numerically, apart from the simple case of  $p = q = 1$  and  $\chi_A = \chi_B = \chi_C$ .

The extent of association  $\Phi$  plays the role of an order parameter for self-assembly and is defined as

$$\Phi \equiv \Phi_C = \frac{\phi_C}{\phi_C(T \rightarrow 0)}, \quad (\text{polymerization upon cooling}) \quad (14)$$

and

$$\Phi \equiv \Phi_C = \frac{\phi_C}{\phi_C(T \rightarrow \infty)}, \quad (\text{polymerization upon heating}) \quad (15)$$

where  $\phi_C(T \rightarrow 0)$  and  $\phi_C(T \rightarrow \infty)$  are the compositions of species C in the low and high temperature limits, respectively. Restricting our attention to association upon cooling, we distinguish three types of behavior for  $\phi_C(T \rightarrow 0)$ . Specifically,

$$\text{if } \frac{\phi_A^\circ}{\phi_B^\circ} = \frac{p}{q},$$

$$\begin{aligned} \phi_A(T \rightarrow 0) = \phi_B(T \rightarrow 0) = 0 \\ \phi_C(T \rightarrow 0) = 1 - \phi_s \end{aligned} \quad (16)$$

$$\text{if } \frac{\phi_A^\circ}{\phi_B^\circ} < \frac{p}{q},$$

$$\begin{aligned} \phi_A(T \rightarrow 0) = 0 \\ \phi_B(T \rightarrow 0) = \phi_B^\circ - \phi_A^\circ(q/p) \\ \phi_C(T \rightarrow 0) = \phi_A^\circ(p+q)/p \end{aligned} \quad (17)$$

$$\text{and if } \frac{\phi_A^\circ}{\phi_B^\circ} > \frac{p}{q},$$

$$\begin{aligned} \phi_A(T \rightarrow 0) = \phi_A^\circ - \phi_B^\circ(p/q) \\ \phi_B(T \rightarrow 0) = 0 \\ \phi_C(T \rightarrow 0) = \phi_B^\circ(p+q)/q \end{aligned} \quad (18)$$

with all limiting values ( $T \rightarrow 0$ ) being independent of  $\{\chi_\alpha\}$ . The definitions in eqs 14 and 15 ensure that  $\Phi_C(T)$  ranges from unity to zero for all compositions  $\phi_A^\circ$  and  $\phi_B^\circ$  and for all values of  $p$  and  $q$ . Alternative definitions of the order parameter follow by analogy with the theory for self-association of a single species, i.e.,

$$\Phi_A = \frac{1 - \phi_A/\phi_A^\circ}{1 - \phi_A(T \rightarrow 0)/\phi_A^\circ} \quad (19)$$

or

$$\Phi_B = \frac{1 - \phi_B/\phi_B^\circ}{1 - \phi_B(T \rightarrow 0)/\phi_B^\circ} \quad (20)$$

These alternative definitions of the order parameter can be shown as exactly coinciding with the definition of  $\Phi_C$ , so a single order parameter  $\Phi \equiv \Phi_A = \Phi_B = \Phi_C$  describes the mutual association process. Equations 16–20 also apply to polymerization upon heating when the limit  $\phi_\alpha(T \rightarrow 0)$  ( $\alpha \equiv A, B, C$ ) is replaced by the limit  $\phi_\alpha(T \rightarrow \infty)$ .

Experimental data for the temperature variation of  $\Phi$  are commonly used to estimate the self-assembly transition temperature, which is determined here as the temperature  $T_\Phi$  at which there is an inflection point in  $\Phi(T)$ , i.e.,  $\partial^2\Phi/\partial T^2|_{\phi_A^\circ, \phi_B^\circ} = 0$ .<sup>57</sup> The function  $T_\Phi = T_\Phi(\phi_{A,n}^\circ)$  is called the association transition line. When solvent is absent from the self-assembling system, (i.e.,  $\phi_s = 0$ ),  $\phi_{A,n}^\circ$  coincides with  $\phi_A^\circ$ .

The average cluster size (mass)  $L$  is another important thermodynamic property for characterizing self-assembly, and its definition naturally extends to mutually assembling systems as

$$L = \frac{n_A + n_B + (p + q)n_C}{n_A + n_B + n_C} = \frac{\phi_A + \phi_B + \phi_C}{\phi_A + \phi_B + \phi_C/(p + q)} = \frac{\phi_A^\circ + \phi_B^\circ}{\phi_A^\circ + \phi_B^\circ - \phi_C(p + q - 1)/(p + q)} \quad (21)$$

where the equilibrium composition  $\phi_C$  is determined by solving eqs 7, 12, and 13. Notice that the unreacted monomers of species A and B are included in the averaging process of eq 21.

Our general model for mutual association reduces to the one-site binding model<sup>2,58</sup> upon setting  $p = q = 1$  and  $\chi_A = \chi_B = \chi_C = \chi_s = 0$  in eqs 7–14, a model widely used in biology and biochemistry.<sup>2,58</sup> Within this model, monomers of species A are ligand molecules that can bind on host molecules B. The fraction  $\theta$  of total binding sites occupied,  $\theta \equiv [AB]/([B] + [AB])$ , defined in the terms of *molar concentrations*  $[\alpha]$  of the reacting species  $\alpha$  ( $\alpha \equiv AB, A, B$ ), is simply the extent of association  $\Phi$  in our single-step mutual association model when  $\phi_A^\circ/\phi_B^\circ > p/q$ . For  $p = q = 1$ , the limit  $\phi_C(T \rightarrow 0) = 2\phi_B^\circ$ , and the extent of association  $\Phi$  of eq 14 reduces to the relation

$$\Phi = \frac{\phi_C}{2\phi_B^\circ} \quad (22)$$

On the other hand, the fraction  $\theta$  equals

$$\theta \equiv \frac{[AB]}{[B] + [AB]} = \frac{(1/2)\phi_C}{\phi_B + (1/2)\phi_C} = \frac{\phi_C}{2\phi_B^\circ} = \Phi \quad (23)$$

Replacing the concentration  $[AB]$  from the expression for the equilibrium constant  $K_c \equiv [AB]/([A][B])$  produces the form

$$\theta = \frac{[A]}{[A] + 1/K_c} \quad (24)$$

that is equivalent to the Langmuir equation for the equilibrium fraction of adsorbed species on a substrate.<sup>59</sup> A plot of  $\theta$  versus  $[A]$  at constant concentration  $[A]_{\text{tot}} \equiv [A] + [AB]$  is then known as the “Langmuir isotherm”. An extension of the one-site binding models to multisite bindings ( $p = n, q = 1$ ) leads to the Hill equation<sup>2</sup>

$$\theta = \frac{[A]^n}{[A]^n + 1/K_c} \quad \text{or} \quad \frac{\theta}{1 - \theta} = \frac{[A]^n}{1/K_c} \quad (25)$$

where the equilibrium constant  $K_c = [A_n B]/([A]^n [B])$  refers to a reaction in which  $n$  ligands A may simultaneously occupy a single receptor B site. The fraction  $\theta$  varies monotonically with concentration  $[A] \equiv c$  of the ligand A and progressively approaches a step function variation as  $n$  is increased toward infinity. (See ref 2 for illustrations of this variation.) A similar jump is also observed in the order parameter  $\Phi$  and signals the onset of a phase transition. The nature of this phase transition will be discussed in another paper focusing on the phase behavior, specific heat, and osmotic properties of mutually associating systems. Because the Hill model<sup>2</sup> coincides with the single-step mutual association model for  $q = 1$  and  $\chi_A = \chi_B = \chi_C = \chi_s = 0$ , our treatment represents an extension of the Langmuir and Hill models to  $p, q > 1$  and to inclusion of the

dependence on nonassociative interactions, a dependence that is essential for describing phase behavior.

**B. Cooperativity Parameter of Mutual Association.** Many basic biological processes rely on regulating the “cooperativity” of mutual association, a property related to the sharpness and selectivity of the association transition as a function of thermodynamic variables such as temperature. The crucial importance of “cooperativity” to mutual association in biology provides the stimulus for intensely investigating this phenomenon.<sup>2,58,60</sup> Hill<sup>2</sup> systematically treated cooperativity in mutual association processes, and we have recently discussed<sup>50</sup> the complementary case of cooperativity in self-association processes. Thus, only a brief summary of the definition of cooperativity is reviewed here.

A prototype of mutual association processes is the binding of oxygen to the four binding sites of hemoglobin in human blood, a process crucial for respiration. Investigation of this problem has been exhaustive,<sup>2–6,58</sup> and the theory for this type of cooperative association process has been generalized to diverse processes involving variations in the configuration and number of binding sites, heterogeneity in the binding site interactions, etc.<sup>2,58</sup> These studies provide a common definition of the “cooperativity” of the binding transition for all mutual association processes. In particular, the “cooperativity index”  $n$  of a ligand binding to  $m$  binding sites is often defined in terms of the rate of change of  $\theta$  in the vicinity of its inflection point<sup>2</sup>

$$n = 4 \left( \frac{\partial \theta}{\partial \ln C} \right)_{\text{inflection point of } \theta(c)} \quad (26)$$

Association processes for which  $n < 1$  are often called “anticooperative”, while those for which  $n > 1$  are termed “cooperative”. For example,  $n$  has been estimated to equal 2.8 for the binding oxygen to hemoglobin,<sup>61</sup> and values of  $n$  as large as 42 have been reported in “ultrasensitive” binding processes.<sup>62,63</sup> The simplest A–B association is perfectly uncooperative for  $n = 1$ . Basically, a large  $n$  signifies that the transition is “sharp”, while maximum cooperativity corresponds to  $n = m$ . As in assembly by self-association,<sup>50</sup> the existence of other chemical equilibria involving the A and B species (e.g., the thermal activation of the species A) constrains the A–B cluster assembly process, which in turn can appreciably change the cooperativity of the association thermodynamics transition.<sup>62,63</sup> Modulation of transition sharpness by such many-body effects plays a large role in many biological switching and sensing processes.<sup>62–64</sup>

**C. Multistep Model of Mutual Association of  $A_p B_q$  Species.** As mentioned in the Introduction, self-assembly often occurs through a hierarchy of processes that may proceed under widely different thermodynamic conditions, allowing for the programmed formation of complex structures composed of relatively simple elementary molecules. For example, the basic building blocks (e.g., triskelion structures of clathrins<sup>23–25</sup> or the pentamer and hexamer protamers of virus capsids<sup>26</sup>) first organize by mutual assembly and then subsequently order into larger scale clusters. Another example of this type of assembly is the linking of two cDNA polymers of different molar mass by gold nanoparticles.<sup>65</sup> The supermolecular organization of antigen–ligand complexes into polymer-like structures provides yet another example of a significant biological multistep self-assembly process.<sup>22</sup> Branched polymeric structures are often observed when the antigen and ligand groups are attached to particles.<sup>14–20</sup>

This subsection describes a simple model in which the complex  $A_p B_q$  is formed as the initial step for further self-

assembly where chain growth proceeds by the subsequent linkage (i.e., polymerization) of  $A_pB_q$  clusters according to the general equation



This second self-assembly process is governed by a different pair of free energy parameters, the enthalpy  $\Delta h_p$  and entropy  $\Delta s_p$  of propagation, which for simplicity are assumed to be independent of  $i$ , so that all successive reactions in eq 27 are characterized by the common equilibrium constant  $K_p$

$$K_p = \exp[-(\Delta h_p - T\Delta s_p)/(k_B T)] \quad (28)$$

A similar model has been considered in connection with the formation of cholesterol–phospholipid complexes.<sup>66</sup> In contrast to the single-step model in which all clusters  $C$  are restricted to have the same size  $p + q$ , the equilibrium system contains species  $\{C_i\} \equiv \{(A_pB_q)_i\}$  of various sizes  $\{i(p + q)\}$  and is thus specified by a richer set of volume fractions  $\phi_A$ ,  $\phi_B$ , and  $\{\phi_{C_i}\}$ . Mass conservation constraints relate these volume fractions to the initial concentrations  $\phi_A^\circ$  and  $\phi_B^\circ$

$$\phi_A^\circ = \phi_A + \frac{p}{p+q} \sum_{i=1}^{\infty} \phi_{C_i} \quad (29)$$

and

$$\phi_B^\circ = \phi_B + \frac{q}{p+q} \sum_{i=1}^{\infty} \phi_{C_i} \quad (30)$$

The Helmholtz free energy is given by a more complicated expression than eq 4

$$\begin{aligned} \frac{F}{N_1 k_B T} = & \phi_s \ln \phi_s + \phi_A \ln \phi_A + \phi_B \ln \phi_B + \\ & \sum_{i=1}^{\infty} \frac{\phi_{C_i}}{i(p+q)} \ln \phi_{C_i} + \sum_{i=1}^{\infty} \phi_{C_i} f_{C_i} + 2\chi_{AB} \phi_A \phi_B + \chi_{AA} \phi_A^2 + \\ & \chi_{BB} \phi_B^2 + 2\chi_{AC} \phi_A \sum_{i=1}^{\infty} \phi_{C_i} + 2\chi_{BC} \phi_B \sum_{i=1}^{\infty} \phi_{C_i} + \\ & \chi_{CC} \left( \sum_{i=1}^{\infty} \phi_{C_i} \right)^2 + 2\chi_{As} \phi_s \phi_A + 2\chi_{Bs} \phi_s \phi_B + 2\chi_{Cs} \phi_s \sum_{i=1}^{\infty} \phi_{C_i} + \\ & \chi_{ss} \phi_s^2 \quad (31) \end{aligned}$$

where  $\{\chi_{\alpha\beta} \propto 1/T\}$  are the interaction parameters between monomers of species  $\alpha$  and  $\beta$  ( $\alpha, \beta \equiv A, B, C, s$ ) and are taken as identical to those in eq 4, since the van der Waals interactions of the clusters  $\{C_i\}$  are assumed to be insensitive to the magnitude of  $i$  (in order to minimize the number of adjustable parameters). The quantity  $f_{C_i}$  in eq 31 is the specific free energy of the species  $C_i$  and is obtained from FH theory for linear polymer chains as

$$f_{C_i} = \frac{1}{i(p+q)} \ln \frac{2\gamma^2}{zi(p+q)} + \frac{i(p+q)-1}{i(p+q)} - \ln \gamma + \frac{i}{i(p+q)} \frac{\Delta h - T\Delta s}{k_B T} + \frac{i-1}{i(p+q)} \frac{\Delta h_p - T\Delta s_p}{k_B T} \quad (32)$$

where  $z$  is the lattice coordination number, the stiffness parameter  $\gamma$  equals unity again for stiff chains and  $z - 1$  for fully flexible chains, and the free energy parameters ( $\Delta h$ ,  $\Delta s$ ) and ( $\Delta h_p$ ,  $\Delta s_p$ ) correspond to the reactions described by eqs 1 and 27, respectively.

The presence of two different association processes also modifies the condition of chemical equilibrium to the form

$$\mu_{C_i} = ip\mu_A + iq\mu_B \quad (33)$$

where the chemical potential  $\mu_{C_i}$  of the species  $C_i$  and the chemical potentials  $\mu_A$  and  $\mu_B$  are determined from eq 31. After some algebra, eq 33 can be transformed into the compact expression for the volume fractions  $\{\phi_{C_i}\}$

$$\phi_{C_i} = i\mathcal{C}\mathcal{A}^i, \quad 0 < \mathcal{A} < 1 \quad (34)$$

with the quantities  $\mathcal{C}$  and  $\mathcal{A}$  expressed as

$$\mathcal{C} \equiv \frac{z(p+q)}{2\gamma^2 K_p} \quad (35)$$

and

$$\mathcal{A} \equiv \phi_A^p \phi_B^q \gamma^{p+q} K K_p \exp[2\phi_A(\chi_A - \chi_C) + 2\phi_B(\chi_B - \chi_C) + 2\phi_s(\chi_s - \chi_C) + 2\chi_C] \quad (36)$$

The interaction parameters  $\chi_A$ ,  $\chi_B$ ,  $\chi_C$ , and  $\chi_s$  of eq 36 are defined by eqs 8–11.

Substituting eq 34 into eqs 29 and 30 and performing all the summations (with the constraint  $0 < \mathcal{A} < 1$ ) yield two important relations

$$\phi_A^\circ = \phi_A + \frac{p}{p+q} \frac{\mathcal{C}\mathcal{A}}{(1-\mathcal{A})^2} \quad (37)$$

and

$$\phi_B^\circ = \phi_B + \frac{q}{p+q} \frac{\mathcal{C}\mathcal{A}}{(1-\mathcal{A})^2} \quad (38)$$

that can be used to express  $\mathcal{A}$  of eq 36 in terms of  $\phi_A^\circ$  and  $\phi_B^\circ$  and finally to determine  $\{\phi_{C_i}\}$  from eq 34 and other basic thermodynamic properties described below.

The extent of polymerization  $\Phi$  is defined similarly to eqs 14 and 15

$$\Phi = \frac{\sum_{i=1}^{\infty} \phi_{C_i}}{\sum_{i=1}^{\infty} \phi_{C_i}(T \rightarrow 0)} = \frac{\mathcal{BA}}{(1 - \mathcal{A})^2},$$

$$\lim_{T \rightarrow 0} \frac{\mathcal{BA}}{(1 - \mathcal{A})^2},$$

polymerization upon cooling (39)

and

$$\Phi = \frac{\sum_{i=1}^{\infty} \phi_{C_i}}{\sum_{i=1}^{\infty} \phi_{C_i}(T \rightarrow \infty)} = \frac{\mathcal{BA}}{(1 - \mathcal{A})^2},$$

$$\lim_{T \rightarrow \infty} \frac{\mathcal{BA}}{(1 - \mathcal{A})^2},$$

polymerization upon heating (40)

while the average cluster size  $L$  equals

$$L = \frac{n_A + n_B + (p + q) \sum_{i=1}^{\infty} i n_{C_i}}{n_A + n_B + \sum_{i=1}^{\infty} n_{C_i}}$$

$$= \frac{\phi_A + \phi_B + \sum_{i=1}^{\infty} \phi_{C_i}}{\phi_A + \phi_B + \sum_{i=1}^{\infty} \phi_{C_i}/i(p + q)}$$

$$= \frac{\phi_A^{\circ} + \phi_B^{\circ}}{\phi_A^{\circ} + \phi_B^{\circ} - \frac{\mathcal{BA}}{(1 - \mathcal{A})^2} + \frac{\mathcal{BA}}{[(1 - \mathcal{A})(p + q)]}} \quad (41)$$

where  $n_{C_i}$  denotes the number of clustered species  $C_i$ .

The fraction  $\Phi_p$  of  $\{A_p B_q\}_i$  clusters that are in the polymerized state ( $i \geq 2$ )

$$\Phi_p = \frac{\sum_{i=2}^{\infty} n_{C_i}}{\sum_{i=1}^{\infty} n_{C_i}} = \frac{\sum_{i=2}^{\infty} \phi_{C_i}/i(p + q)}{\sum_{i=1}^{\infty} \phi_{C_i}/i(p + q)} = \mathcal{A} \quad (42)$$

is the order parameter for the polymerization process. Similarly, the average size  $L_p$  of clusters  $\{A_p B_q\}_i$  is expressed as

$$L_p = \frac{(p + q) \sum_{i=1}^{\infty} i n_{C_i}}{\sum_{i=1}^{\infty} n_{C_i}} = \frac{\sum_{i=1}^{\infty} \phi_{C_i}}{\sum_{i=1}^{\infty} \phi_{C_i}/i(p + q)} = \frac{p + q}{1 - \mathcal{A}} \quad (43)$$

### III. Results

This section summarizes calculations of basic thermodynamic observables of the single-step and multistep models of mutual association. These basic properties include the order parameters

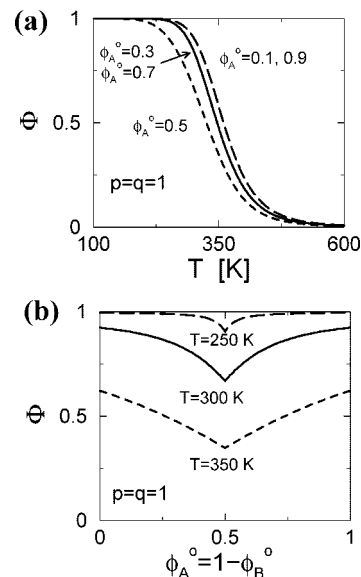


**Figure 1.** The order parameter  $\Phi$  for the single-step mutual association as a function of temperature  $T$  for various initial concentrations  $\phi_A^0$  of species A and as a function of the initial volume fraction  $\phi_A^0$  for various temperatures  $T$  (b). The associating complexes  $A_p B_q$  are assumed to consist of single molecules of species A and B, i.e.,  $p = q = 1$ .

for mutual association ( $\Phi$ ) and polymerization ( $\Phi_p$ ), the compositions  $\phi_A$ ,  $\phi_B$ , and  $\phi_C$ , the polymerization transition lines  $T_\Phi(\phi_A^0, n)$ , and the average cluster size  $L$ . All calculations are performed assuming that the associating species are rigid, i.e., by setting the stiffness parameter  $\gamma$  in eqs 7, 35, and 36 to unity, since no qualitative changes ensue for the fully flexible case. The enthalpy  $\Delta h$  and entropy  $\Delta s$  associated with the reaction in eq 1 are selected as  $\Delta h/(p + q - 1) = -35$  kJ/mol and  $\Delta s/(p + q - 1) = -105$  J/(mol K), consistent with our previous choice in studies of self-association.<sup>57</sup> The same values are ascribed to the enthalpy  $\Delta h_p = -35$  kJ/mol and entropy  $\Delta s_p = -105$  J/(mol K) of polymerization of the  $\{A_p B_q\}$  complexes. Negative values of  $\Delta h$ ,  $\Delta s$ ,  $\Delta h_p$ , and  $\Delta s_p$  imply that self-assembly occurs upon cooling in the illustrative examples below. The theory described in section II can also be applied to a system exhibiting self-assembly upon heating. Because the thermodynamic properties mentioned above (but not the phase separation and osmotic properties) depend only weakly on the interaction parameters  $\{\chi_{\alpha\beta}\}$  ( $\alpha, \beta \equiv A, B, C, s$ ), the effective parameters  $\{\chi_\alpha\}$  are set to zero in the current illustrative calculations. The lattice coordination number  $z$  is taken as  $z = 6$ , corresponding to a three-dimensional simple cubic lattice.

**A. Calculations for the Single-Step Model of Mutual Association. 1. Order Parameter  $\Phi$ .** The numerical analysis of the  $\mathcal{M}\mathcal{A}_{pq}$  model begins by considering the simplest system comprising unreacted monomers A and B, symmetric clusters AB ( $p = q = 1$ ), and no solvent ( $\phi_s = 0$ ). Figure 1a exhibits the extent of polymerization  $\Phi$  for this mixture as a function of temperature  $T$  for series of different initial concentrations  $\phi_A^0$ . The general temperature variation of the extent of polymerization  $\Phi$  is common to both mutual and self-assembly upon cooling:  $\Phi(T, \phi_A^0 = \text{const})$  is a sigmoidal function that approaches unity at low temperatures and zero at high temperatures. Moreover,  $\Phi(T)$  in Figure 1a is identical for volume fractions  $\phi_A^0$  and  $1 - \phi_A^0$ , and the minimum in  $\Phi(T = \text{const})$  occurs for  $\phi_A^0 = 0.5$ . These features are evident consequences of the symmetry under exchange of the particle labels A and B and are also apparent in Figure 1b, which presents  $\Phi$  as a function of

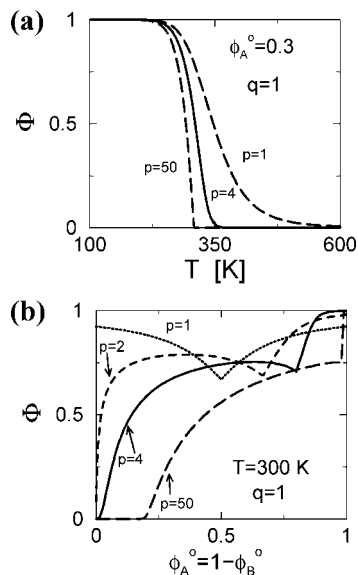


**Figure 2.** The order parameter  $\Phi$  for the single-step mutual association ( $q = 1$  and variable stoichiometric index  $p$ ) as a function of temperature  $T$  for fixed initial volume fraction  $\phi_A^0 = 0.3$  of species A (a) and as a function of the initial volume fraction  $\phi_A^0$  at a fixed temperature  $T = 300$  K (b).

composition  $\phi_A^0$  for several fixed temperatures. The nonmonotonic variation of  $\Phi$  with  $\phi_A^0$  and the decreasing  $\Phi(T = \text{const}, \phi_A^0)$  over a certain composition range are characteristics that distinguish mutual association from self-association.

Lifting the symmetry condition  $p = q$  qualitatively alters the variation of  $\Phi$  with temperature and composition, as exemplified by Figure 2a and b for a system which departs from that analyzed in Figure 1a and b only by allowing the index  $p$  to be variable. Figure 2a indicates that increasing  $p$  ( $p > q = 1$ ) leads to a steeper function  $\Phi(T, \phi_A^0 = \text{const})$  and to a sharper association transition. Physically more relevant features are displayed by Figure 2b where  $\Phi$  is analyzed as a function of  $\phi_A^0$ . Removing the compositional symmetry of AB complexes causes  $\Phi(T = \text{const}, \phi_A^0)$  to exhibit a rather flat maximum in addition to the sharp minimum. The composition at which  $\Phi(T = \text{const}, \phi_A^0)$  is minimum shifts from  $\phi^* = 0.5$  (intrinsic to the  $p = q$  case) to the stoichiometric concentration  $\phi^* = p/(p + q)$ . Consequently, the left and right branches of  $\Phi(T = \text{const}, \phi_A^0)$  are asymmetric. When  $p$  and  $q$  differ considerably, the critical association transition concentration<sup>67</sup>  $\phi_c \equiv (\phi_A^0)^{(c)}$  departs significantly from zero (for instance,  $\phi_c \approx 0.2$  for  $p = 50$  and  $q = 1$  in the example illustrated in Figure 2b), and the compositions corresponding to the maximum and minimum of  $\Phi(T = \text{const}, \phi_A^0)$  approach each other.

One underemphasized aspect of mutual association is its sensitivity to dilution, which we now examine. The presence of solvent complicates the description of the system because two independent concentration variables [e.g.,  $\phi_{A,n}^0 \equiv \phi_A^0/(1 - \phi_s)$  and  $\phi_s$ ] are necessary to uniquely specify the system's composition. Parts a and b of Figure 3 describe the influence of dilution on the order parameter  $\Phi$  by exhibiting  $\Phi(T, \phi_{A,n}^0 = \text{const})$  and  $\Phi(\phi_{A,n}^0, T = \text{const})$ , respectively, for several volume fractions  $\phi_s$ . Both figures refer to the simplest  $p = q = 1$  system and indicate that dilution does not qualitatively alter the temperature and composition variations of  $\Phi(T, \phi_{A,n}^0)$  but instead substantially decreases  $\Phi(T = \text{const})$  and  $\Phi(\phi_{A,n}^0 = \text{const})$ . Thus, the addition of solvent leads to a sharper association transition, i.e., to an increased cooperativity as defined by eq 26.

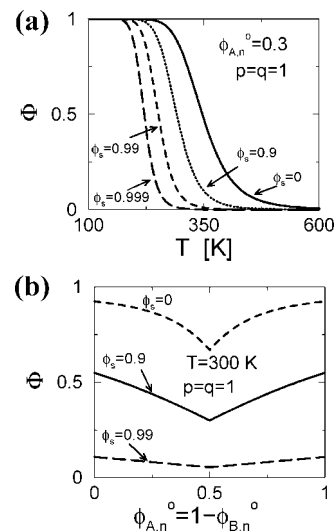


**Figure 3.** The order parameter  $\Phi$  for the single-step mutual association ( $p = q = 1$ ) as a function of temperature  $T$  for fixed normalized initial concentration  $\phi_{A,n}^0 \equiv \phi_A^0/(1 - \phi_s) = 0.3$  of species A (a) and as a function of the initial volume fraction  $\phi_{A,n}^0$  for fixed temperature  $T = 300$  K (b). Different curves correspond to different volume fractions  $\phi_s$  of the solvent.

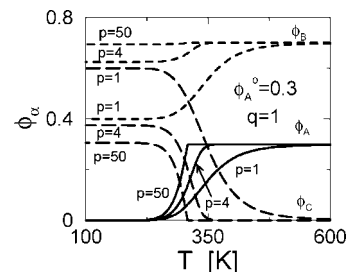


**Figure 4.** Temperature variation of the concentrations  $\phi_A$  (solid line),  $\phi_B$  (dashed line), and  $\phi_{C=A_p B_q}$  (long dashed line) for the single-step mutual association mixture with fixed initial volume fraction  $\phi_A^0 = 0.3$  of species A and with no solvent ( $\phi_s = 0$ ). Different curves correspond to different stoichiometric indices  $p$  and a common stoichiometric index  $q = 1$ .

## 2. Concentrations $\phi_A$ , $\phi_B$ , and $\phi_C$ of Species A, B, and C.

While the order parameter  $\Phi$  generally quantifies the overall degree of mutual assembly, the individual concentrations of the mutually associating species provide deeper insights. This subsection describes the concentrations profiles  $\{\phi_\alpha(T, \phi_A^0)\}$  ( $\alpha \equiv A, B, C$ ) for the simplest case where the volume fraction  $\phi_s$  vanishes and  $q = 1$ . Figure 4 illustrates  $\{\phi_\alpha\}$  as a function of temperature  $T$  for fixed initial concentration  $\phi_A^0 = 0.3$  and various  $p = 1, 4, \text{ and } 50$ . The choice  $\phi_A^0 = 0.3$  implies that B is the majority component (i.e.,  $\phi_B^0 = 0.7$ ). Consequently,  $\phi_A$ ,  $\phi_B$ , and  $\phi_C$  range, respectively, from limits of zero,  $(0.7 - 0.3/p)$ , and  $\phi_A^0(p + 1)/p$  at low temperatures to limits of  $\phi_A^0$ ,  $\phi_B^0$ , and zero at high temperatures (see eqs 16–18 for recovering these limits). More careful inspection of Figure 4 reveals that larger  $p$  (i.e., a larger difference  $p - q$ ) imparts a stronger temperature variation to the concentrations  $\phi_A$  and  $\phi_C$  but a weaker temperature dependence to the concentration of the majority species ( $\phi_B$ ). If  $p - q$  is sufficiently large (e.g.,  $p - q = 49$  as in Figure 4),  $\phi_B$  hardly varies with temperature.

Complementary information about the dependence of the concentrations  $\phi_A$ ,  $\phi_B$ , and  $\phi_C$  on the initial monomer volume fraction  $\phi_A^0$  emerges from Figure 5. Figure 5a displays  $\{\phi_\alpha\}$  ( $\alpha \equiv A, B, C$ ) vs  $\phi_A^0$  for the  $p = q = 1$  system and two temperatures  $T = 250$  K and  $T = 300$  K. While  $\phi_A$  grows from zero to unity



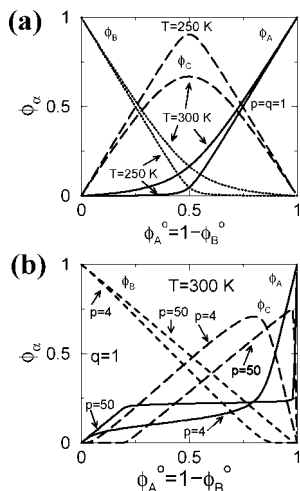


**Figure 5.** Concentrations  $\phi_A$  (solid line),  $\phi_B$  (dashed line), and  $\phi_{C=A_pB_q}$  (long dashed line) as a function of the initial volume fraction  $\phi_A^0$  for the single-step mutual association system with  $p = q = 1$  (a) and with  $q = 1$  and a variable  $p$  (b). Different curves correspond to different temperatures and to different values of  $p$ .

and  $\phi_B$  decreases from unity to zero over the whole range of  $\phi_A^0$ , the concentration  $\phi_C$  exhibits a maximum (whose magnitude depends on temperature  $T$ ) at the symmetrical concentration  $\phi^* = 0.5$ . Figure 5b extends Figure 5a to asymmetric systems ( $p > q = 1$ ) and demonstrates that the maximum in  $\phi_C(T)$  shifts from  $\phi^* = 0.5$  to  $\phi^* = 0.8$  when  $p = 4$  and  $q = 1$  and to near unity ( $\phi^* \approx 0.98$ ) when  $p = 50$  and  $q = 1$ . The maximum of  $\phi_C(T)$  thus appears at the identical concentration  $\phi^*$  to that for which  $\Phi(T=\text{const}, \phi_A^0)$  is minimum (see Figure 2b). Interestingly,  $\phi_A$  remains practically unchanged over a large range of  $\phi_A^0$  (from around 0.2 to around 0.98) and then jumps rapidly to unity.

**3. Self-Assembly Transition Lines  $T_\Phi(\phi_{A,n}^0)$  and  $T_\Phi(\phi_A^0)$ .** As already mentioned, the polymerization transition temperature  $T_p$  for a given  $\phi_A^0$  (or  $\phi_{A,n}^0$  when solvent is present) is very often identified with the temperature  $T_\Phi$  at which the order of parameter  $\Phi$  exhibits an inflection point, i.e., where  $\partial^2\Phi/\partial T^2|_{\phi_A^0, \phi_B^0} = 0$ . The resulting curve  $T_\Phi(\phi_A^0)$  [or  $T_\Phi(\phi_{A,n}^0)$ ] represents the boundary between A and B monomer-rich and  $A_pB_q$  complex-rich “states”, and  $T_\Phi(\phi_A^0)$  is thus called the “association transition line”. We first analyze these lines for the solvated  $p = q = 1$  system ( $\phi_s \neq 0$ ) in Figure 6a which illustrates the changes in  $T_\Phi(\phi_{A,n}^0)$  with dilution. First of all, dilution diminishes the mutual association transition temperature  $T_\Phi$ . Second, the computed association transition lines in Figure 6a resemble the order parameter curves  $\Phi(T=\text{const}, \phi_{A,n}^0)$  in Figure 3b. All the transition lines have a minimum at the symmetric concentration  $(\phi_{A,n}^0)^* = 0.5$ , in contrast to the polymerization transition lines for self-association that grow monotonically with concentration (when self-association proceeds upon cooling).<sup>57</sup> Figure 6b exhibits the influence of dilution on  $T_\Phi$  from a different perspective by considering the temperature  $T_\Phi$  as a function of  $\phi_s$  for fixed  $\phi_{A,n}^0$ . The sharp decline of the association transition temperature  $T_\Phi$  with increasing  $\phi_s$  is more accentuated than in Figure 6a.

Figure 7 addresses the important issue of how the “association line”  $T_\Phi(\phi_A^0)$  alters with the stoichiometric indices of the  $A_pB_q$  complexes by considering systems with no solvent ( $\phi_s = 0$ ), variable index  $p$ , and fixed  $q = 1$ . The formation of unsymmetric complexes  $A_pB_q$  qualitatively changes the association transition line by the appearance of a maximum in addition to the minimum in  $T_\Phi(\phi_A^0)$ , which generally occurs at the stoichiometric concentration  $\phi^* = p/(p+q)$ . Likewise, the resemblance

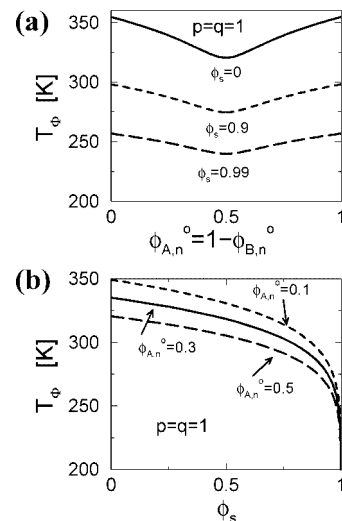


**Figure 6.** Self-assembly transition temperature  $T_\Phi$  for the single-step mutual association model ( $p = q = 1$ ) as a function of the normalized initial reduced volume fraction  $\phi_{A,n}^0 \equiv \phi_A^0/(1 - \phi_s)$  of species A (a) and as a function of the volume fraction  $\phi_s$  of the solvent (b). Different curves in parts a and b correspond, respectively, to different volume fractions  $\phi_s$  of the solvent and to different initial volume fractions  $\phi_{A,n}^0$  of species A.

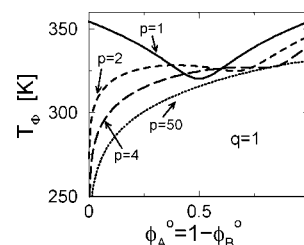


**Figure 7.** Self-assembly transition temperature  $T_\Phi$  for a single-step mutual association model as a function of the initial volume fraction  $\phi_A^0$  of species A. Different curves correspond to different values of the stoichiometric index  $p$ , while the second stoichiometric index is fixed as  $q = 1$ .

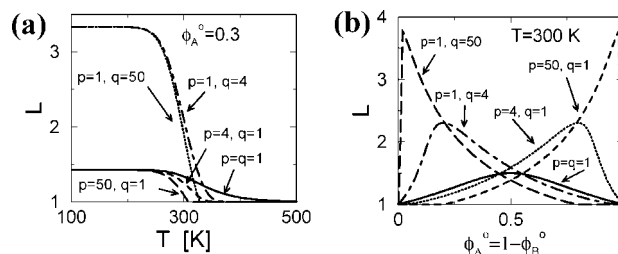


**Figure 8.** The average cluster size  $L$  for a single-step mutual association model as a function of temperature  $T$  for fixed initial volume fraction  $\phi_A^0 = 0.3$  of species A (a) and as a function of the concentration  $\phi_A^0$  for fixed temperature  $T = 300$  K (b). Different curves correspond to different pairs of the stoichiometric indices  $p$  and  $q$ .

between the association transition lines  $T_\Phi(\phi_A^0)$  for the  $p = q = 1$  mixtures and the order parameter curves  $\Phi(\phi_A^0)$  of Figure 2b is striking.

**4. Average Cluster Size  $L$ .** The average cluster size  $L$  strongly affects the transport properties of associating systems. When the free energy parameters  $\Delta h$  and  $\Delta s$  of the reaction in eq 1 and the effective interaction parameters  $\{\chi_\alpha\}$  of eqs 8–11 are fixed, the average cluster size  $L$  depends on temperature  $T$ , volume fractions  $\phi_A^0$  and  $\phi_s$ , and the stoichiometric indices  $p$  and  $q$ . For simplicity, our illustrative calculations of  $L$  described below are performed for systems with no solvent ( $\phi_s = 0$ ).

Figure 8a presents the average cluster size  $L$  as a function of temperature  $T$  for fixed initial volume fraction  $\phi_A^\circ = 0.3$  and various combinations of  $p$  and  $q$ . While the differences in the  $L(T)$  curves for  $q = 1$  and variable  $p$  (or vice versa) over a wide temperature range are in accord with general expectations, the existence of a common low temperature limit for all the curves (see Figure 8a) is not as obvious. This result, however, follows by substituting the low temperature limit  $\phi_C(T \rightarrow 0)$  from eqs 16–18 into the expression for  $L$  in eq 21 (specialized for  $\phi_s = 0$ ), thereby obtaining

$$L(T \rightarrow 0) = \frac{1}{1 - \frac{(p+q-1)}{p+q} \phi_C(T \rightarrow 0)} = \frac{1}{1 - \frac{(p+q-1)}{p} \phi_A^\circ}, \quad \text{if } \frac{\phi_A^\circ}{\phi_B^\circ} < \frac{p}{q} \quad (44)$$

$$L(T \rightarrow 0) = \frac{1}{1 - \frac{(p+q-1)}{p+q} \phi_C(T \rightarrow 0)} = \frac{1}{1 - \frac{(p+q-1)}{q} \phi_B^\circ}, \quad \text{if } \frac{\phi_A^\circ}{\phi_B^\circ} > \frac{p}{q} \quad (45)$$

and

$$L(T \rightarrow 0) = \frac{1}{1 - \frac{(p+q-1)}{p+q} \phi_C(T \rightarrow 0)} = \frac{1}{1 - \frac{(p+q-1)}{p+q}} = p+q, \quad \text{if } \frac{\phi_A^\circ}{\phi_B^\circ} = \frac{p}{q} \quad (46)$$

When  $q = 1$ , eq 44 reduces to

$$L(T \rightarrow 0) = \frac{1}{1 - \phi_A^\circ}, \quad \text{if } \frac{\phi_A^\circ}{\phi_B^\circ} < p \quad (47)$$

whereas when  $p = 1$ , eq 45 simplifies to the relation

$$L(T \rightarrow 0) = \frac{1}{\phi_A^\circ}, \quad \text{if } \frac{\phi_A^\circ}{\phi_B^\circ} > 1/q \quad (48)$$

Equations 47 and 48 demonstrate that the low temperature limit of  $L$  depends only on  $\phi_A^\circ$  when one of the indices  $p$  and  $q$  equals 1, thereby explaining the trends seen in Figure 8a.

For completeness, Figure 8b illustrates the average cluster size  $L$  as a function of the initial concentration  $\phi_A^\circ$  for fixed temperature  $T = 300$  K and the same pairs of  $p$  and  $q$  as in Figure 8a. The average cluster size  $L$  exhibits a peak at  $\phi^* = p/(p+q)$  whose magnitude grows with decreasing temperature for association upon cooling. The curves for  $L(T = \text{const}, \phi_A^\circ)$  are mirror reflections upon exchange of the indices  $p$  and  $q$ .

**B. Calculations for the Multistep Model of Mutual Association.** The multistep assembly model is specified by two pairs of free energy parameters ( $\Delta h$ ,  $\Delta s$ ) and ( $\Delta h_p$ ,  $\Delta s_p$ ) that are

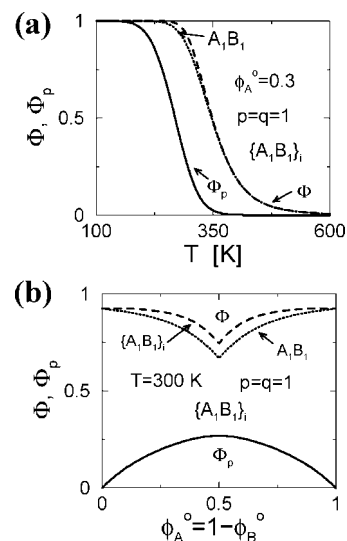


**Figure 9.** The order parameters  $\Phi$  and  $\Phi_p$  for the multistep mutual association as a function of temperature  $T$  for fixed initial concentration  $\phi_A^\circ$  of species A (a) and as a function of the volume fraction  $\phi_A^\circ$  for fixed temperature  $T = 300$  K (b). Both parts refer to the hierarchical  $p = q = 1$  system.

assumed to be identical and equal to  $\Delta h_p = \Delta h = -35$  kJ/mol and  $\Delta s_p = \Delta s = -105$  kJ/mol in our illustrative calculations. Since many thermodynamic properties of multistep and single-step models of mutual association exhibit similar trends, the discussion here is restricted to properties that differ between these two models or that are only specific for the multistep model.

The fraction  $\Phi_p$  of the  $\{A_p B_q\}$  clusters existing in the polymerized state quantifies the extent of polymeric ordering, and  $\Phi_p$  is compared to the order parameter  $\Phi$  for the formation of the mutual association complexes in Figure 9 for symmetrical associating complexes AB (i.e.,  $p = q = 1$ ) and for a system without a solvent ( $\phi_s = 0$ ). Figure 9a indicates that  $\Phi_p(T, \phi_A^\circ = \text{const})$  lies in a lower temperature region than  $\Phi(T, \phi_A^\circ = \text{const})$ , illustrating that the ordering processes occur through *sequential steps* upon cooling, the essence of *temperature programmed assembly*.<sup>65</sup> The actual temperature variations of  $\Phi$  and  $\Phi_p$  are similar, but the transition temperatures are well separated. Specifically,  $\Phi_p(T, \phi_A^\circ = \text{const})$  has a well defined inflection point at the temperature  $T_{\Phi_p}$  which is significantly smaller than the self-assembly transition temperature  $T_\Phi$ . Thus, a system where associating complexes can further polymerize is described by two separate transition lines  $T_{\Phi_p}(\phi_A^\circ)$  and  $T_\Phi(\phi_A^\circ)$ . The gap between these two lines increases for  $|\Delta h_p| < |\Delta h|$ . While  $\Phi_p(T, \phi_A^\circ = \text{const})$  and  $\Phi(T = \text{const}, \phi_A^\circ)$  are qualitatively similar, the composition variations of  $\Phi_p$  and  $\Phi$  differ, as shown in Figure 9b. The order parameter  $\Phi(T = \text{const}, \phi_A^\circ)$  is minimum at  $\phi^* = 0.5$ , while  $\Phi_p(T = \text{const}, \phi_A^\circ)$  exhibits a maximum at the same concentration  $\phi^*$ . A similar parabolic upward shape of  $\Phi_p(T = \text{const}, \phi_A^\circ)$  is maintained when  $p$  differs from  $q$ , as illustrated in Figure 10 for several temperatures and  $p = 10$  and  $q = 1$ . A maximum occurs at the same concentration  $\phi^* = p/(p+q) \approx 0.9091$  for all temperatures considered in Figure 10. The separation between the transition lines can be tuned by varying the enthalpy and entropy of mutual association and polymerization with respect to each other.

The average cluster size  $L$  also differs significantly between single-step and multistep models and is analyzed for the latter model in Figures 11 and 12 for a system with no solvent ( $\phi_s = 0$ ). Parts a and b of Figure 11 present  $L$  as a function of temperature  $T$  for various initial concentrations  $\phi_A^\circ$  (and  $p = q = 1$ ) and for various pairs of  $p$  and  $q$  (and fixed  $\phi_A^\circ = 0.3$ ), respectively. While

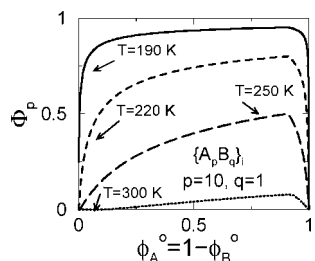


**Figure 10.** The order parameter  $\Phi_p$  as a function of the initial concentration  $\phi_A^0$  of species A for the multistep association ( $p = 10$ ,  $q = 1$ ). Different curves correspond to different temperatures.

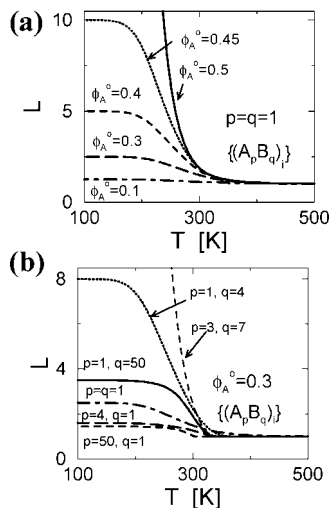


**Figure 11.** The temperature variation of the average cluster size  $L$  for the multistep mutual association mixture ( $p = q = 1$ ) for different initial concentrations  $\phi_A^0$  of species A (a) and for fixed  $\phi_A^0 = 0.3$  and various pairs of the stoichiometric indices  $p$  and  $q$  (b).

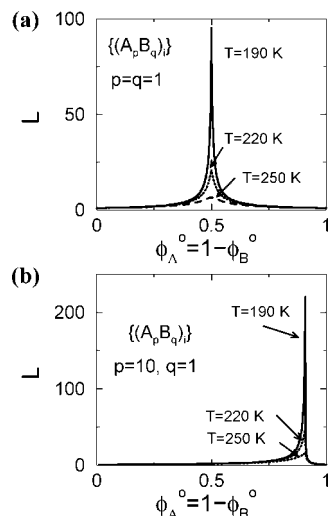


**Figure 12.** The average cluster size  $L$  for the multistep mutual association mixture as a function of the initial concentration  $\phi_A^0$  of species A for various temperatures. Parts a and b refer to  $p = q = 1$  and  $p = 10$  and  $q = 1$ , respectively.

$L$  at low temperatures is always finite for the single-step model (see Figure 8), the low temperature limit  $L(T \rightarrow 0)$  of  $L$  for the multistep model diverges at the stoichiometric concentration  $\phi^* = p/(p + q)$

$$L(T \rightarrow 0, \phi_A^0 = \phi^*) = \infty \quad (49)$$

The average cluster size  $L$  for concentrations other than  $\phi^*$  saturates at low temperatures to a plateau (see Figure 11) whose magnitude depends on  $\phi_A^0$  and the indices  $p$  and  $q$ . Figure 12 emphasizes the nontrivial low temperature behavior of  $L(\phi_A^0, T = \text{const})$ , demonstrating that the average size (mass) of the clusters that form by polymerization of the mutual association complexes can be quite large and that this cluster growth tends to peak exactly at the stoichiometric concentration  $\phi^* = p/(p + q)$ .

Particle clustering should evidently strongly affect the transport and thermodynamic properties of these fluids. For example, the solution viscosity varies linearly with mass for untangled polymers and with a substantially higher power law exponent ( $\approx 3.4$ ) for entangled polymers.<sup>68</sup> A sharp increase in the cluster size  $L$  should reflect itself in the viscosity as a function of composition, and numerous observations reveal corresponding maxima in the viscosity (and the low frequency dielectric constant) of polymer–solvent mixtures.<sup>35</sup> Figure 13 presents an extreme example of this sharp maximum for mixtures of allythiocarbamide and diethylamine and of allythiocarbamide and methylaniline,<sup>35</sup> that arises from strong mutual association of these species. The resemblance of Figures 12 and 13 is striking. Similar maxima in the shear viscosity as a function of composition are also reported for polyelectrolytes<sup>69,70</sup> and for mixtures of polar and polyelectrolyte polymers.<sup>51</sup> The latter class of systems is of recent interest in connection with the fabrication of extremely tough gels when one of the polymers is cross-linked. A cusplike composition variation is also apparent for the glass transition temperature  $T_g$  of associating mixtures, since  $T_g$  depends appreciably on the polymer molar mass when the molecular mass is low or moderate. For instance,  $T_g$  for a mixture of chlorinated hydrocarbons with organic bases exhibits a cusplike variation as in Figure 13 due to the formation of large mutual association complexes.<sup>42</sup>

#### IV. Discussion

Many biological structures self-assemble by a combination of complex formation and the subsequent polymerization of the complexes into larger scale clusters, a process that can produce intricate hierarchical structures. The basic complex units form through highly specific, complementary interactions between the associating species, while their mutual anisotropic interactions enable their organization into larger scale self-assembling structures. Recent interest centers on emulating these hierarchical biological self-assembly processes for material synthesis.<sup>14–20</sup> In particular, highly selective mutual association processes provide an attractive vehicle for creating functional nanostructures<sup>14–20</sup> and for programming assembly processes through a series of alterations in thermodynamic variables, such as temperature.<sup>65</sup> The present paper initiates a systematic study of hierarchical self-assembly with an emphasis on the thermodynamics of complex formation by mutual association and then on situations where the complexes, in turn, exhibit their own self-assembly, generating perhaps the simplest example of programmed self-assembly. In order to focus on generic characteristics of the self-assembly, the particular mechanism of complex formation is not considered. (Ercolani's<sup>49</sup> treatment of complex formation addresses the detailed nature of the intra- and intermolecular associative contacts, which can be important in modeling particular associative systems.) The basic thermodynamic properties examined here are of importance to both theory and experiment and include the order parameters  $\Phi$  and  $\Phi_p$  for the self-assembly transitions, the average cluster mass  $L$ , the concentrations (e.g.,  $\phi_C$ ) of the individual species, and the dependence of these quantities on temperature and the initial system's composition.

Our previous series of papers<sup>50,67,71</sup> describes a systematic investigation of the thermodynamics of self-assembly that proceeds

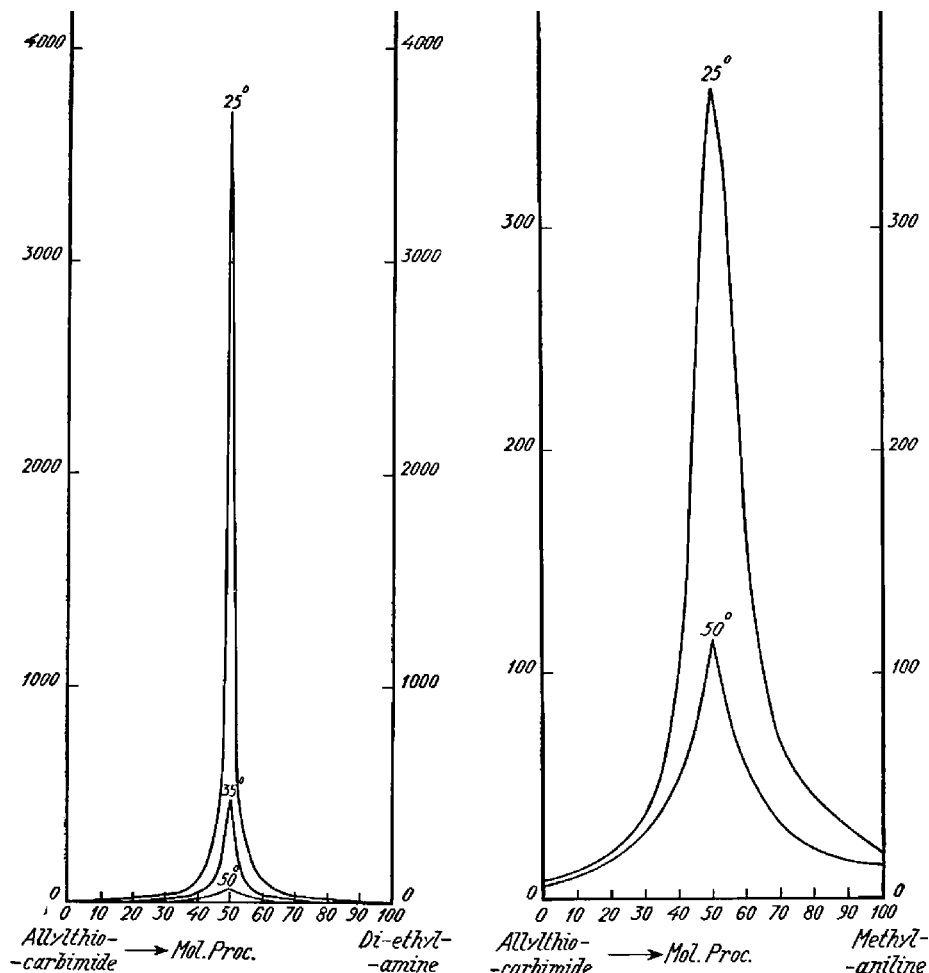


**Figure 13.** Shear viscosity of allylthiocarbimide–diethylamine and allylthiocarbimide–methylaniline binary mixtures as a function of composition at various temperatures. Reprinted from ref 35 with permission. Copyright 1938 Nordemann Publ. Co., Inc. The viscosity units in the left and right figures are 10 poise and  $10^3$  poise, respectively (1 poise = 0.1 Pa·s).

by *self-association* in which cluster growth occurs exclusively by combining molecules of a single kind. While the temperature variations of basic thermodynamic properties are rather similar for mutual association and self-association systems, *qualitative* changes appear in their composition dependence. In contrast to self-association where  $\Phi$ ,  $\phi_C$ ,  $L$ , or the transition temperature  $T_\Phi$  change monotonically with composition, a nonmonotonic variation of these properties is intrinsic to self-assembly by mutual association. Specifically,  $\Phi(T=\text{const}, \phi_\lambda^*)$  and  $T_\Phi(\phi_\lambda^*)$  have minima, whereas  $\phi_C(T=\text{const}, \phi_\lambda^*)$  and  $L(T=\text{const}, \phi_\lambda^*)$  display maxima, and these extrema occur at the same critical stoichiometric concentration  $\phi^* = p/(p + q)$ . These extrema and those observed in the viscosity and other transport properties are signatures for this type of mutual assembly process.

Allowing the mutually associated species to self-assemble in a hierarchical fashion generates a hybrid model that shares features of both the mutual and self-association models. This multistep mutual association model is characterized by two order parameters, the second of which,  $\Phi_p$ , quantifies the polymerization process of the  $A_pB_q$  complexes. Our calculations indicate that the second self-assembly transition temperature  $T_{\Phi_p}$ , where  $\partial^2\Phi_p/\partial T^2 = 0$ , is well separated from the transition temperature  $T_\Phi$  (for complex formation), where  $\partial^2\Phi/\partial T^2 = 0$ , even when  $\Delta h_p = \Delta h$  and  $\Delta s_p = \Delta s$  are identical for both processes. Moreover, the composition dependence of  $\Phi_p$  and  $\Phi$  qualitatively differs (see Figures 9b and 10), but the minimum of  $\Phi(T=\text{const}, \phi_\lambda^*)$  and the maximum of  $\Phi_p(T=\text{const}, \phi_\lambda^*)$  again appear at the same stoichiometric concentra-

tion,  $\phi^* = p/(p + q)$ . When the association complexes themselves can polymerize, the average cluster size  $L$  (mass) can become very large, as illustrated in Figure 12. Similar peaks are reported<sup>35</sup> in the concentration dependence of the shear viscosity for binary mixtures of strongly mutually associating species. Moreover, when the relative initial concentration  $\phi_\lambda^2/\phi_\beta^2$  coincides with the stoichiometric ratio  $p/q$ , the average cluster size  $L(T, \phi_\lambda^2 = \text{const})$  can even diverge at low temperatures (see Figure 11).

The majority of our illustrative calculations summarized in section III apply to systems in which solvent is absent and all nonassociative interactions are ignored because the properties considered are either independent or weakly dependent on the van der Waals interactions. However, the theory in section II is formulated to enable the calculation of many other thermodynamic properties (e.g., critical parameters for phase separation or osmotic quantities) that strongly depend on the signs and magnitudes of the effective interaction parameters  $\{\chi_\alpha\}$  of eqs 8–11. Since previous papers<sup>57,71</sup> demonstrate the existence of a strong coupling between self-association and phase separation, similar qualitative changes in phase behavior are expected for mutually associating fluids. McConnell and co-workers<sup>27,53</sup> have already shown examples of this dramatic coupling, such as phase diagrams with multiple upper critical solution critical points, in the context of modeling of cholesterol and phospholipid complexes in membranes.

The presence of solvent in mutually associating systems is often ignored, but we find that solvent can appreciably impact the thermodynamics of mutual assembly. Figures 3 and 6 indicate that

both the order parameter  $\Phi$  and the transition temperature  $T_\Phi$  for association change with the system's dilution. Moreover, the average cluster size  $L$  (mass) and all other properties likewise depend on solvent concentration  $\phi_s$ . The dependence on  $\phi_s$  found from our theory also implies a dependence of the thermodynamic properties on pressure, and the current theory may be generalized readily to treat compressible systems, albeit at the expense of increasing the number of model parameters. Thus, our underlying theory may provide significant extensions of the classic Langmuir and Hill models that are widely applied in biology and biochemistry.

**Acknowledgment.** The paper is supported, in part, by NSF grant number CHE-0749788 and by the Joint Theory Institute which is funded by Argonne National Laboratory and the University of Chicago.

## References and Notes

- Bongrand, P. *Rep. Prog. Phys.* **1991**, *62*, 921.
- Hill, T. L. *Cooperativity Theory in Biochemistry*; Springer Series in Molecular Biology; Springer-Verlag: New York, 1985. See also: Gibson, R. E.; Levin, S. A. *Proc. Natl. Acad. Sci.* **1977**, *74*, 139.
- Pauling, L. *Proc. Natl. Acad. Sci.* **1935**, *21*, 186.
- Hopfield, J. J. *Nobel* **1973**, *24*, 238.
- Riggs, A. F. *EMBO J.* **2003**, *22*, 4980.
- Royer, W. E.; Zhu, H.; Gorr, T. A.; Flores, J. F.; Knapp, J. E. *J. Biol. Chem.* **2005**, *280*, 27477.
- Fisher, E. *Ber. Dtsch. Chem. Ges.* **1894**, *27*, 2984. This classic paper has been translated in Lemieux, U. R.; Spohr, U. *Adv. Carbohydr. Chem. Biochem.* **1994**, *50*, 1. For a modern discussion of the lock and key model and its generalization to account for protein flexibility, see: Koshland, D. E., Jr. *Angew. Chem. Int. Ed.* **1995**, *33*, 2375.
- Ptashne, M. *Philos. Trans. R. Soc. London* **2003**, *361*, 1223. Veitia, R. A. *Biol. Rev.* **2003**, *78*, 149. Lundstrom, P. A. *Biophys. Chem.* **2001**, *94*, 1.
- Nam, Y.; Sliz, P.; Pear, W. S.; Aster, J. C.; Blacklow, S. C. *Proc. Natl. Acad. Sci.* **2007**, *104*, 2103.
- Gale, E. F. *The Molecular Basis of Antibiotic Action*, 2nd ed.; John Wiley: London, 1981.
- Gilli, P.; Ferretti, V.; Gilli, G.; Borea, P. A. *J. Phys. Chem.* **1994**, *98*, 1515.
- Lehn, J. M. *Proc. Natl. Acad. Sci.* **2002**, *99*, 4763.
- Hof, F.; Rebek, J., Jr. *Proc. Natl. Acad. Sci.* **2002**, *99*, 4775.
- Shenton, W.; Davis, S. A.; Mann, S. *Adv. Mater.* **1999**, *11*, 449.
- Caswell, K. K.; Wilson, J. N.; Bunz, U. H. F.; Murphy, C. J. *J. Am. Chem. Soc.* **2003**, *125*, 13914.
- Mirkin, C. A. *Inorg. Chem.* **2000**, *39*, 2258.
- Goshe, A. J.; Steele, I. M.; Cecciarelli, C.; Rheingold, A. L.; Bosnich, B. *Proc. Natl. Acad. Sci.* **2002**, *99*, 4823.
- Tanton, T. A.; Mirkin, C. A.; Letsinger, R. L. *Science* **2000**, *289*, 1757.
- Mirkin, C. A.; Letsinger, R. L.; Mucic, R. C.; Storhoff, J. J. *Nature* **1996**, *382*, 607.
- Alivisatos, A. P.; Johnsson, K. P.; Peng, X.; Wilson, T. E.; Loweth, C. J.; Bruchez, M. P., Jr.; Schultz, P. G. *Nature* **1996**, *382*, 609.
- Nykypanchuk, D.; Maye, M. M.; van der Lelie, D.; Gang, O. *Nature* **2008**, *451*, 549.
- Zhang, Y.; Gu, H.; Yang, Z.; Xu, B. *J. Am. Chem. Soc.* **2003**, *125*, 13680.
- Murphy, R. M.; Slayter, H.; Schurtenberger, P.; Chamberlin, R. A.; Colton, C. K.; Yarmush, M. L. *Biophys. J.* **1988**, *54*, 45.
- Crowther, R. A.; Pearse, S. F. *J. Cell Biol.* **1981**, *91*, 790.
- Kirchhausen, T. *Annu. Rev. Biochem.* **2002**, *69*, 699.
- Nossal, R. *Macromol. Symp.* **2005**, *219*, 1.
- Prevelige, P. E., Jr.; Thomas, D.; King, J. *Biophys. J.* **1993**, *64*, 824.
- Radhakrishnan, A.; Anderson, T. G.; McConnell, H. M. *Proc. Natl. Acad. Sci.* **2000**, *97*, 12422.
- Kotera, M.; Lehn, J.-M.; Vigneron, J. P. *J. Chem. Soc.: Chem. Comm.* **1994**, 197.
- Sherrington, D. C.; Taskinen, K. A. *Chem. Soc. Rev.* **2001**, *30*, 83.
- Hirst, A. R.; Smith, D. K.; Feiters, M. C.; Geurts, H. P. M.; Wright, A. *J. Am. Chem. Soc.* **2003**, *125*, 9010.
- Kalomiets, E.; Buhler, E.; Candau, S. J.; Lehn, J.-M. *Macromolecules* **2006**, *39*, 1173.
- Lee, H. Y.; Nam, S. R.; Hong, J.-I. *J. Am. Chem. Soc.* **2007**, *129*, 1040.
- Feldman, K. E.; Kade, M. J.; de Greef, T. F. A.; Meijer, E. W.; Kramer, E. J.; Hawker, C. J. *Macromolecules* **2008**, *41*, 4694. Berl, V.; Schmutz, M.; Krische, M. J.; Khoury, R. G.; Lehn, J.-M. *Chem.—Eur. J.* **2002**, *8*, 1227.
- Noro, A.; Matsushita, Y.; Lodge, T. P. *Macromolecules* **2008**, *41*, 5839.
- Jaeger F. M. *Second Report on Plasticity*; Nordemann Publ.: New York, 1938; pp 81–82, Chapter II.
- Rasmussen, D. H.; McKenzie, A. P. *Nature* **1968**, *220*, 1315.
- Schichman, S. A.; Amey, R. L. *J. Phys. Chem.* **1971**, *75*, 98. Matsui, T.; Hopler, L. G.; Fenby, D. V. *J. Phys. Chem.* **1973**, *77*, 2397.
- Cowie, J. M. G.; Toporowski, P. M. *Can. J. Chem.* **1961**, *39*, 2240.
- Luzar, A. *J. Mol. Fluids* **1990**, *46*, 221.
- Luck, W. A. P. *J. Mol. Struct.* **1998**, *448*, 131.
- Dougan, L.; Bates, S. P.; Hargreaves, R.; Fox, J. P.; Crain, J.; Finney, J. L. *J. Chem. Phys.* **2004**, *121*, 6456.
- Lesikar, A. V. *J. Phys. Chem.* **1976**, *80*, 1005; *J. Chem. Phys.* **1977**, *66*, 4263; **1975**, *63*, 2297.
- Muthukumar, M. *J. Chem. Phys.* **2004**, *120*, 9343.
- Levin, Y. *Physica A* **1999**, *66*, 413.
- Goswami, M.; Kumar, S. K.; Bhattacharya, A.; Douglas, J. F. *Macromolecules* **2007**, *40*, 4113.
- Garces, J. L.; Mas, F. *J. Chem. Phys.* **1999**, *111*, 2818.
- Bekiranov, S.; Bruinsma, R.; Pincus, P. *Phys. Rev. E* **1997**, *55*, 577.
- Koehler, R. D.; Raghavan, S. R.; Kaler, E. W. *J. Phys. Chem. B* **2000**, *104*, 11035.
- Ercolani, G. *J. Am. Chem. Soc.* **2003**, *125*, 16097; *J. Phys. Chem. B* **2003**, *107*, 5052; *Struct. Bonding (Berlin)* **2006**, *121*, 167.
- Douglas, J. F.; Dudowicz, J.; Freed, K. F. *J. Chem. Phys.* **2008**, *128*, 224901.
- Tominaga, T.; Tirumala, V. R.; Gong, J. P.; Furukawa, H.; Osada, Y.; Lin, E. K.; Wu, W.-L. *Polymer* **2007**, *48*, 7449.
- Tirumala, V. R.; Tominaga, T.; Lee, S.; Butler, P. D.; Lin, E. K.; Furukawa, H.; Gong, J. P.; Osada, Y.; Wu, W.-L. *J. Phys. Chem. B* **2008**, *112*, 8024.
- Radhakrishnan, A.; McConnell, H. M. *J. Am. Chem. Soc.* **1999**, *121*, 486; *Biophys. J.* **1999**, *77*, 1507.
- Olaussen, K.; Stell, G. *J. Stat. Phys.* **1991**, *62*, 221.
- Debye, P. *J. W. Ann. N.Y. Acad. Sci.* **1949**, *51*, 575.
- Artyomov, M. N.; Freed, K. F. *J. Chem. Phys.* **2005**, *123*, 194906.
- Dudowicz, J.; Freed, K. F.; Douglas, J. F. *J. Chem. Phys.* **2003**, *119*, 12645.
- Koshland, D. E., Jr.; Nemethy, G.; Filmer, D. *Biochemistry* **1966**, *5*, 365.
- Karpovich, D. S.; Blanchard, G. *J. Langmuir* **1994**, *10*, 3315.
- Wyman, J.; Gill, S. J. *Binding and Linkage: Functional Chemistry of Biological Macromolecules*; University Science Books: Mill Valley, CA, 1990.
- Stryer, L. *Biochemistry*; Freeman: New York, 1995.
- Ferrell, J. E., Jr.; Machleder, E. M. *Science* **1998**, *280*, 895.
- Koshland, D. E., Jr. *Science* **1998**, *280*, 852. Koshland, D. E., Jr.; Goldbeter, A.; Stock, J. B. *Science* **1982**, *217*, 220.
- Veita, R. A. *Biol. Rev.* **2003**, *78*, 149.
- Dillenback, L. M.; Goodrich, G. P.; Keating, C. D. *Nano Lett.* **2006**, *6*, 16.
- Anderson, T. G.; McConnell, H. M. *Biophys. J.* **2002**, *83*, 2039.
- Dudowicz, J.; Freed, K. F.; Douglas, J. F. *J. Chem. Phys.* **1999**, *111*, 7116. Douglas, J. F.; Dudowicz, J.; Freed, K. F. *J. Chem. Phys.* **2007**, *127*, 224901.
- Doi, M.; Edwards, S. F. *The Theory of Polymer Dynamics*; Clarendon Press: 1988.
- Ganter, J. L. M. S.; Milas, M.; Rinaudo, M. *Polymer* **1992**, *33*, 113.
- Cohen, J.; Priel, Z.; Rabin, Y. *J. Chem. Phys.* **1992**, *88*, 7111; **1990**, *93*, 9062.
- Dudowicz, J.; Freed, K. F.; Douglas, J. F. *J. Chem. Phys.* **2000**, *112*, 1002; **2000**, *113*, 434. Rah, K.; Freed, K. F.; Dudowicz, J.; Douglas, J. F. *J. Chem. Phys.* **2006**, *124*, 144906.